Collective excitations in liquid ^{4}He: I. Experiment and presentation of data

1994 J. Phys.: Condens. Matter 6 821

(http://iopscience.iop.org/0953-8984/6/4/003)

J. Phys.: Condens. Matter 6 (1994) 821–834. Printed in the UK

Collective excitations in liquid ^{4}He: I. Experiment and presentation of data

K H Andersen†‡§, W G Stirling‡, R Scherm‖†, A Stunault‖¶, B Fåk† ††, H Godfrin† ‡‡ and A J Dianoux†

† Institut Laue–Langevin, BP 156X, 38042 Grenoble Cédex 9, France
‡ Department of Physics, School of Science and Engineering, Keele University, Keele, Staffordshire ST5 5BG, UK
‖ Physikalisch-Technische Bundesanstalt, Bundesallee 100, Postfach 3345, 3300 Braunschweig, Germany
†† Centre d'Etudes Nucléaires de Grenoble, 85X, 38041 Grenoble Cédex, France
‡‡ Centre de Recherches sur les Très Basses Températures, CNRS, BP 166X, 38402 Grenoble Cédex, France

Received 7 July 1993, in final form 15 October 1993

Abstract. We report neutron scattering measurements of the dynamic structure factor $S(Q, \omega)$ of liquid ^{4}He in the collective excitation regime. The use of the IN6 time-of-flight spectrometer at the Institut Laue–Langevin has enabled us to cover the wavevector region from 0.3 to 2.1 Å^{-1} in a continuous manner with an accurately calibrated energy scale and an energy resolution of approximately 0.1 meV; temperatures between 1.24 and 4.95 K were examined at saturated vapour pressure. In the wavevector region investigated, sharp excitations are seen that are unique to superfluid ^{4}He; it is the purpose of the present paper to examine their temperature dependence and to discuss measurements of the multiphonon continuum scattering at higher energies. At small wavevectors in the 'phonon' region, the excitations are relatively unaffected by the lambda transition, whereas at larger Q a sharp component disappears at or close to T_λ. The temperature variation of $S(Q, \omega)$ is much more rapid in the superfluid phase than in the normal phase. In paper II of this series, the results for $S(Q, \omega)$ will be compared with several models for the temperature variation of the ^{4}He excitation spectrum.

1. Introduction

Since the discovery of the superfluid properties of liquid ^{4}He below the lambda transition, this fluid has continued to attract both theoretical and experimental interest. Landau (1941) first proposed that collective excitations would exist in liquid ^{4}He due to the strong interactions between the helium atoms. In his later work (Landau 1947) he predicted that the elementary 'phonon–roton' density excitations would have a linear sound-mode dispersion at small wavevector Q with, at larger Q, a quadratic 'roton minimum'. Numerous experimental studies of the collective excitations of superfluid ^{4}He have been carried out, notably employing the techniques of thermal neutron scattering (see, for example, Cowley and Woods (1971) and Woods and Cowley (1973)); these have confirmed the qualitative shape of the dispersion curve proposed by Landau and developed by Feynman (1954) and by

§ Current address: Booster Synchrotron Utilization Facility, National Laboratory for High Energy Physics, 1-1 Oho, Tsukuba-shi, Ibaraki-ken, 305 Japan.

¶ Current address: European Synchrotron Radiation Facility, BP 220, 38043 Grenoble Cédex, France.

0953-8984/94/040821+14$07.50

Feynman and Cohen (1956). A comprehensive review of work on the excitation spectrum of liquid ^{4}He up to 1987, covering both theoretical and experimental aspects, has been given by Glyde and Svensson (1987).

At low temperatures, the dynamic structure factor $S(Q, \omega)$ of liquid ^{4}He is seen to consist of a single sharp peak, following the well known phonon–maxon–roton dispersion curve; hereafter, this single excitation peak is referred to as the 'one-phonon' peak at all wavevectors examined. At energies above the one-phonon peak a broad region of scattering is observed, which is normally attributed to multiphonon excitations. Calculations in the ground state of the liquid (Manousakis and Pandharipande 1986) have now reached a stage where excellent agreement is obtained with the dynamic structure factor measured by neutron scattering techniques.

Until recently, however, the temperature dependence of $S(Q, \omega)$ has not been well understood. The phonon excitations in liquid ^{4}He are unique in remaining sharply defined up to a wavevector in excess of 3 Å^{-1} in the superfluid phase. This suggests that they are in some way connected to the presence of a Bose condensate, but demonstrating this microscopically has proved difficult. Woods and Svensson (1978) suggested a decomposition of the scattering function into parts arising from the normal and superfluid components. They applied the procedure to data taken at saturated vapour pressure (SVP) and showed that the temperature dependence of $S(Q, \omega)$ was well described over the measured wavevector range between 0.8 and 2.0 Å^{-1}. The excitation energies and lifetimes extracted from the superfluid component of $S(Q, \omega)$, using their procedure, were in better agreement with theoretical calculations (e.g. Landau and Khalatnikov 1949) than parameters extracted from the total $S(Q, \omega)$. The Woods–Svensson (WS) decomposition is intuitively appealing, but lacks a theoretical basis. Attempts by Talbot and Griffin (1984; and references therein) to provide a microscopic justification have not been successful.

More recently, Talbot *et al* (1988) analysed their new data taken at a pressure of 20 bar, using the Woods–Svensson procedure. They found that $S(Q, \omega)$ did not separate naturally into normal and superfluid components, as the subtraction of a normal fluid component gave rise to negative scattering intensities arising from the superfluid, at some energies, which is not physically meaningful. These experiments did confirm, however, that the sharp component of the scattering function decreases rapidly as the lambda point is approached from low temperatures and disappears or changes abruptly in character at T_λ. Further support for these ideas was provided by the detailed measurements of Stirling and Glyde (1990) who demonstrated the contrasting temperature dependences of phonon ($Q = 0.4$ Å^{-1}) and roton ($Q = 1.925$ Å^{-1}) excitations at SVP. A recent interpretation by Glyde and Griffin (1990) describes, for the first time, the temperature dependence of $S(Q, \omega)$ within a solid theoretical framework. The linear-dispersion part of the spectrum is seen as consisting mainly of a zero-sound mode, similar to that observed in Fermi liquids, while the maxon and roton excitations arise from the excitation of a single quasi-particle. The single-particle excitations are coupled to the density fluctuations by the presence of a non-zero Bose condensate. They thus establish the connection between the Bose broken symmetry and the sharp one-phonon excitations seen in the superfluid phase.

The principal aim of the present experiment was to study the temperature variation of $S(Q, \omega)$ of liquid ^{4}He over a wide range of temperatures and wavevectors, with high resolution, statistical precision and accuracy. Most previous work has followed a rather fragmentary approach in which, for example, phonon measurements are followed by a study of the roton region under conditions of very different resolution and precision. Triple-axis crystal spectrometers have normally been used which provide pointwise information. These instruments are most suited to examine small parts of (Q, ω) space with high resolution.

So, although many different triple-axis measurements have been reported (see Glyde and Svensson 1987) it has not been possible to make detailed comparisons of information obtained under varying resolution conditions.

The current measurements employed the IN6 time-of-flight spectrometer at the Institut Laue–Langevin (ILL), which combines high incident flux with high resolution, to cover *simultaneously* a large part of the collective excitation region of the (Q, ω) plane. The data obtained allow a systematic treatment of the temperature and wavevector dependence of the scattering function of liquid ^{4}He. A subsidiary aim of this study was to provide tabulated information for $S(Q, \omega)$ as a function of temperature and pressure under identical resolution conditions; the energy scale of the spectrometer was calibrated to a relative error of $\sim 10^{-3}$. The present paper describes the first part of this systematic determination. Preliminary accounts of parts of this work have been published elsewhere (Stirling 1991, Andersen *et al* 1992).

The paper is laid out as follows. In section 2, the experimental details are presented along with a brief description of the calibration measurements. Section 3 describes the data reduction procedure followed to obtain $S(Q, \omega)$ from the raw data, whilst a presentation of the results is made in section 4. The multiphonon spectrum is discussed in section 5 and conclusions follow in section 6.

Paper II of this series (Andersen and Stirling 1994) (hereafter referred to as paper II) presents the lineshape analysis employed and describes the determination of the instrumental resolution function from the low-temperature data. The temperature variation of the one-phonon parameters (frequency, width, strength), with due allowance for instrumental resolution, is then discussed in the light of the Woods–Svensson decomposition (Woods and Svensson 1978) and the simple multiphonon subtraction procedure (Miller *et al* 1962). The implications of the current results for the new model due to Glyde and Griffin (1990) are then considered; these ideas are developed in detail in the recent book by Griffin (1993). Paper II concludes with a short discussion section.

2. Experimental details and spectrometer calibration

High-purity ^{4}He was condensed into a cylindrical Al sample cell with an internal volume of approximately 18 cm^3 which was cooled in a helium-flow cryostat (base temperature $\sim$ 1.2 K). Cd spacers were spaced vertically inside the cell to minimize multiple scattering, and the sample temperature was monitored using a calibrated carbon resistor attached to the cell. Quoted temperatures are estimated to be accurate to ± 0.02 K. This was verified by dividing out the Bose thermal population factor $n_B(\omega, T)$ from the measured $S(Q, \omega)$ at constant Q. The resulting spectra should be proportional to the imaginary part of the dynamical susceptibility $\chi(Q, \omega)$ which is symmetric about zero energy transfer (Lovesey 1984). Inaccuracies in the temperature scale would give rise to an asymmetry in this quantity. The results of this procedure confirmed the quoted precision in temperature.

The experiment was performed on the IN6 time-of-flight spectrometer (Blanc 1983), situated on a cold neutron guide tube at the ILL, which provides a very high flux of monochromatic neutrons from three vertically focusing pyrolytic graphite monochromators. There is a continuous detector bank covering scattering angles ϕ from 10° to 115°. Scattering from the walls and heat shields of the cryostat was suppressed by an oscillating collimator placed between the sample and the detectors. A fixed incident neutron energy of 3.8 meV resulted in a resolution width (FWHM) of approximately 0.10 meV, which varies by less than 20% over the relevant range of Q and ω. The instrumental resolution function was

determined using the low-temperature helium data, as discussed in paper II. The results for $S(Q, \omega)$ presented here include the broadening arising from instrumental resolution. A vanadium incoherent scatterer was used to obtain the detector efficiencies used in the data analysis procedure. The incident energy of 3.8 meV was chosen so as to cover a large part of the phonon–roton dispersion curve with as high a resolution as possible. The region of (Q, ω) space covered with the present experimental configuration is shown in figure 1; excitations with SVP wavevectors of between 0.3 and 2.1 $Å^{-1}$ could be examined.

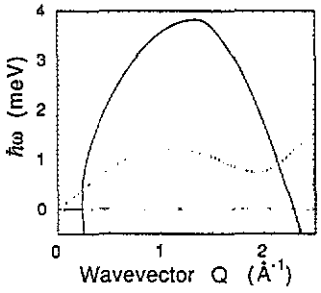

Figure 1. The region of (Q, ω) space covered in the neutron inelastic scattering measurements described in this paper is contained within the full curve. The dotted curve indicates the ^{4}He phonon–roton dispersion curve.

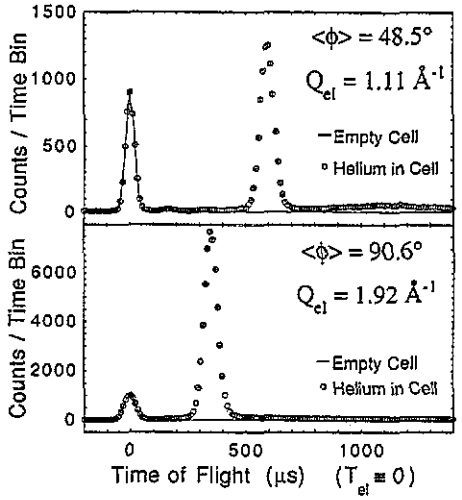

Figure 2. Upper part: raw time-of-flight data corresponding to the maxon wavevector $Q_{ELASTIC}$ = 1.11 $Å^{-1}$; sum of scattering angles ϕ from 47.73° to 49.29°. The open circles show the scattering with liquid helium at SVP and T = 1.30 K in the sample cell, the full curve is the empty-cell scattering. Lower part: as above for the roton wavevector $Q_{ELASTIC}$ = 1.92 $Å^{-1}$; ϕ = 88.92° to 92.32°.

The Al sample cell gives rise to an elastic peak in the measured spectra, which must be subtracted to determine the helium scattering. For this purpose, a run with the empty can was recorded before the ^{4}He runs. Another empty-can measurement was taken half-way through the experiment, and as these two runs showed no systematic differences, they were added together to improve the counting statistics.

The scattering function of liquid ^{4}He was measured at 15 different temperatures between 1.24 and 4.95 K at SVP. An additional measurement at T = 1.24 K was recorded at a pressure of 15 bars.

Since one aim of this work was to provide accurate tabulated data for $S(Q, \omega)$ at several temperatures, particular attention was paid to the calibration of the IN6 time-of-flight spectrometer. The flight paths in the spectrometer were accurately measured in a series of calibration experiments, and the incident beam wavelength and pulse arrival time at the sample were also measured in order to calibrate the energy scale of the spectrometer. As described by Stunault *et al* (1992), the incident wavelength for a narrow beam from the central monochromator was accurately determined using a monitor detector placed 'down stream' from the IN6 sample position. From the time-of-flight measured at a number of

different monitor positions a wavelength of 4.634 ± 0.001 Å was obtained. A cylindrical vanadium sample was then used in conjunction with a NaI gamma-ray detector to determine the time at which prompt capture-gammas emerged from the vanadium; this gives an accurate measurement of the arrival time of neutron pulses at the sample position. Then, by measuring the arrival time of the neutron pulses at the IN6 detectors, the distances to each detector could be determined with an estimated accuracy of about 1 mm. These effective distances vary between 2.467 and 2.475 m across the large detector bank, nominally at 2.483 m.

A second vanadium calibration sample consisting of three concentric cylinders was then inserted in the cryostat at the position to be taken by the ^{4}He sample cell. A procedure was followed to obtain values for the neutron wavelength for each individual detector with the full (three-monochromator) neutron beam. The values found in this way were close to being constant for all detectors, with systematic deviations arising from differences in sample geometry between the sample–detector distance measurements (small beam) and the full-beam measurements. A weighted mean wavelength of 4.630 ± 0.003 Å was obtained and was used in subsequent data analysis.

For calibration of the wavevector scale, the angular positions of the detectors must be known. By visual inspection the IN6 detector boxes were estimated to be at the nominal values to within less than 5 mm laterally, corresponding to an uncertainty in the angular position $\sim 0.1°$ and in wavevector $Q \sim 0.01$ Å^{-1} at a scattering angle of 90°. Further details of the calibration procedure are given in Stunault *et al* (1992) and in Andersen (1991). The accuracy obtained in the energy scale is of the order of 0.002 meV at a typical energy transfer of 1 meV.

3. Data reduction

Figure 2 shows examples of the raw (constant scattering angle, ϕ) data corresponding to the maxon ($Q_{\mathrm{ELASTIC}} = 1.11$ Å^{-1}; a sum of spectra for angles between 47.7° and 49.3°; 'angles' means the centres of the relevant detector boxes) and roton ($Q_{\mathrm{ELASTIC}} = 1.92$ Å^{-1}; a sum of spectra between 88.9° and 92.3°) parts of the dispersion curve presented as a function of neutron time-of-flight; the empty-can scattering is shown as full curves. In order to transform data of this format into $S(Q, \omega)$, the standard time-of-flight data reduction procedure was followed (see, for example, Windsor (1981)), to transform first to $S(\phi, \omega)$; a number of second-order corrections, described below, were then applied to eliminate systematic errors from the data before rebinning to give $S(Q, \omega)$.

The scattering obtained from the empty-sample-cell run was directly subtracted from the observed scattering. This procedure correctly subtracts the time-independent background. However, due to sample-dependent attenuation of the scattering from the Al cell, it gives rise to small systematic errors, comparable in size to the statistical errors in the data. As these effects are confined to the region of the elastic peak, they do not affect the subsequent lineshape analysis.

Frame-overlap effects are caused by neutrons losing so much energy in the scattering process at the sample that they appear in one of the following time frames, due to their low speed. They will then appear to arrive at a time corresponding to a much lower energy transfer. A small correction was made for this effect by fitting a background of the form t^{-4} (where t is the neutron time-of-flight) to the end of the time frame and subtracting its extension into the following frame. The t^{-4} dependence arises from the conversion from time-of-flight to energy, including the neutron wavevector dependence of the inelastic cross

section (Lovesey 1984). This is the form expected for the frame overlap if $S(Q, \omega)$ is flat (Svensson *et al* 1976, Stirling 1990) in the energy range corresponding to neutrons arriving in the subsequent time frame.

For absolute normalization, we extracted $Z(Q)$, the intensity of the one-phonon peak and, using a single scale factor for the entire wavevector range, we scaled the $Z(Q)$ to match that previously measured by Cowley and Woods (1971). We were not able to normalize directly to $S(Q)$, as for most of the measured Q-region the data did not cover a wide enough range in energy to include all of the scattering. The $Z(Q)$ extracted from our constant scattering angle were corrected for the effects of the Jacobian (Waller and Frömann 1952), which are important when the peaks are not measured along lines of constant Q in $(Q$–$\omega)$-space. The $S(Q)$ obtained from our data is consistent with previous neutron and x-ray measurements (Svensson *et al* 1980, Hallock 1972). More details of the data reduction procedure are to be found in Andersen (1991).

The accuracy of the energy scale can be tested by a comparison of the measured dispersion curve with previous high-accuracy (triple-axis) measurements. For the low-temperature runs, the position of the sharp peak was obtained for each $S(\phi, \omega)$ spectrum by a Gaussian fit, and a parabolic dispersion curve was fitted to the results for wavevectors at the roton minimum. The roton parameters (the roton gap Δ, the roton wavevector Q_R, and the roton effective mass μ_R) have been accurately measured on triple-axis spectrometers (Woods *et al* 1977, Stirling 1991), and the best-fit roton parameters obtained from the present data (Andersen *et al* 1992) are presented in table 1. There is excellent agreement between the current values, those previously determined, and those given in the compilation by Donnelly *et al* (1981). Roton parameters extracted using the Woods–Svensson model are discussed in paper II.

Table 1. Roton parameters, Δ (the roton gap), Q_R (the roton wavevector) and μ_R (the roton effective mass) from the present study compared with previous determinations and compilations.

T (K)	Δ (K)	Q_R (Å^{-1})	μ_R(^{4}He)
0.05[a]	8.608 (±0.01)	1.920 (±0.002)	0.136 (±0.005)
0.75[b]	8.618 (±0.009)	1.926 (±0.005)	0.126 (±0.030)
0.90[a]	8.605 (±0.010)	1.924 (±0.002)	0.150 (±0.005)
'Low'[c]	8.616	1.930	0.153
1.24[d]	8.622 (±0.015)	1.931 (±0.003)	0.144 (±0.003)
1.30[d]	8.615 (±0.015)	1.930 (±0.003)	0.141 (±0.003)

[a] Stirling (1991).
[b] Woods *et al* (1977).
[c] Donnelly *et al* (1981).
[d] This work.

In order to perform quantitative comparisons with previous data (mostly from triple-axis spectrometers), or with theoretical calculations, the data are more useful in constant-Q form. An algorithm was devised which performs a rebinning of the data taken along lines of constant scattering angle in the (Q, ω) plane onto a rectangular (Q, ω) grid. This algorithm is based on the fact that the detectors are very close together and thus the strip in the (Q, ω) plane described by each detector can be approximated as touching the neighbouring strips. The constant-Q strip onto which the data are to be rebinned is chosen to have a width in Q which is substantially larger than the Q-width of each detector. The measured data points are then rebinned onto the constant-Q strip, weighted by their overlap area. Being a 'rebinning' procedure, rather than a least-squares fit, the transformation from constant

scattering angle to constant Q is *unique*, and depends only on the widths chosen for the Q and ω bins. As demonstrated in figure 1 the neutron kinematical restrictions result in energy ranges which vary widely over the wavevector range. The data were rebinned into constant-Q representations of width 0.05 $Å^{-1}$ over the entire measured range. Over the sharp one-photon peaks the energy bin width was 0.02 meV, whilst away from the well defined excitations an energy bin of 0.05 meV was employed. The scattering function $S(Q, \omega)$ obtained as described above is available elsewhere in tabulated form†.

4. Presentation of data

In figure 3 we present the $T = 1.30$ K data rebinned to constant Q at representative wavevectors. At each wavevector the sharp one-phonon excitation is accompanied, at higher energy, by wide multiphonon scattering (Cowley and Woods 1971) which exhibits significant structure. This part of the spectrum is discussed in more detail in section 5. In order to estimate how much of the 'multiphonon' intensity is due to multiple scattering, the semi-analytic method of Sears (1975a) was employed. The ratio of double-to-single scattering depends on the sample geometry and was found to be 2.5%, interpolated from table 5 of Sears (1975b). The full curves of figure 3 show the calculated multiple-scattering contribution, which is seen to be small and increasingly negligible as Q increases. The structure in the scattering at energies above the one-phonon peak is thus primarily of multiphonon origin and has been observed in previous studies (Stirling 1985, 1990). We note that the multiple-scattering contribution is always negligible in the region of the one-phonon peak. None of the data presented in this paper have had multiple-scattering contributions subtracted.

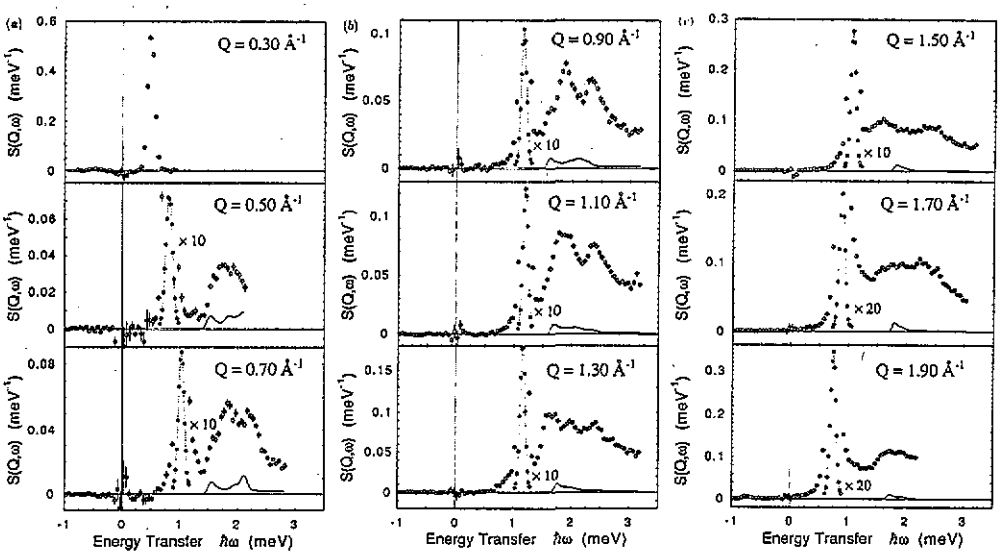

Figure 3. Corrected data at selected constant wavevectors Q; $S(Q, \omega)$ at SVP and $T = 1.30$ K. For presentation purposes the sharp one-phonon peak intensity has been divided by the scale factor shown. The full curves present the calculated multiple-scattering contribution.

† Tables lodged with British Library under reference number SUP70049.

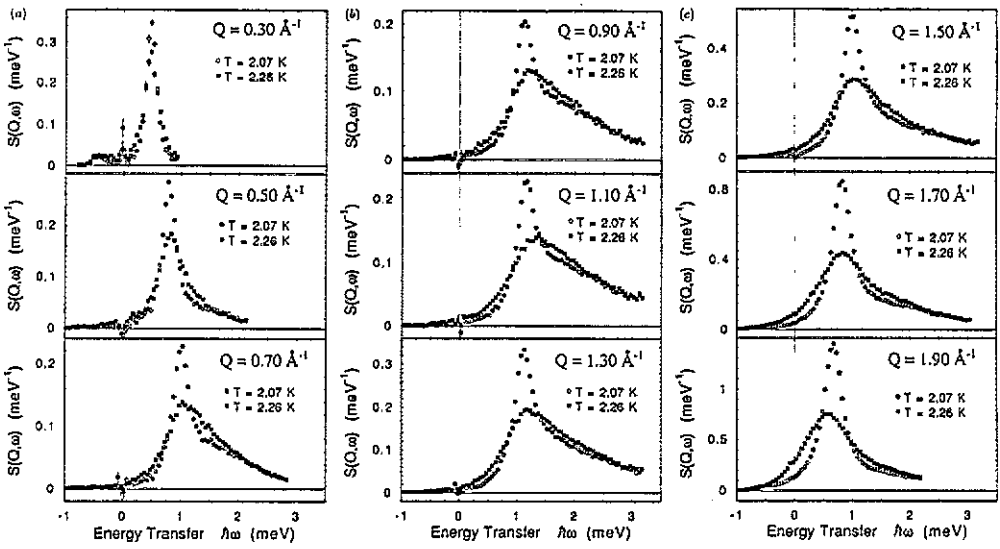

Figure 4. Corrected SVP data at constant Q; $S(Q,\omega)$ for two temperatures just below ($T = 2.07$ K) and just above ($T = 2.26$ K) T_λ.

Figure 4 shows the rebinned data at temperatures of 2.07 and 2.26 K, just below and just above T_λ at the same wavevectors as figure 3. While the most obvious effect at low Q is a line broadening, the higher Q data ($Q > 0.7$ Å^{-1}) demonstrate that there is a qualitative difference in the spectra below and above the lambda point. This will be discussed more fully below. At the highest temperature investigated (4.95 K), where the SVP is close to 2 bar, the inelastic spectra are broad and featureless; the FWHM lie between 1 and 2 meV. These data will not be discussed further here since systematic measurements of $S(Q,\omega)$ at 4.2 K have been reported and tabulated by Woods *et al* (1978), covering the range 0.1 to 10 Å^{-1}.

With such a large body of data describing $S(Q,\omega)$ at many temperatures, contour or (hidden-line) three-dimensional representations can significantly assist with the presentation of results. The temperature dependence of the observed $S(Q,\omega)$ is exemplified by figures 5 to 7, where the scattering function at wavevectors of 0.40 (phonon), 1.20 (maxon), and 1.90 Å^{-1} (roton), are shown in three-dimensional representations of $S(Q,\omega,T)$ at constant Q. We note that, for clarity, the data used to produce these figures have been smoothed and so they provide only qualitative illustrations of the temperature variation of the scattering. The temperature dependence in the low-Q phonon region appears simple. The scattering consists of a single, sharp peak, which broadens with temperature; the multiphonon component is relatively weak and well separated from the single excitation peak. The rate of broadening of the one-phonon peak appears to change at or near T_λ, but a well-defined peak remains visible in the normal fluid phase. At the maxon wavevector, the low-temperature scattering function is seen to consist of a sharp peak, superimposed on a broad multiphonon 'background', which changes little with temperature. The sharp peak, however, is seen to disappear at T_λ, suggesting that it is in some way a 'signature' of the superfluid phase, connected to the existence of the Bose condensate. The situation is similar at the roton wavevector. Here the sharp peak is also seen to disappear at T_λ and the scattering in the normal phase is peaked at an energy (~ 0.5 meV), lower than that of the

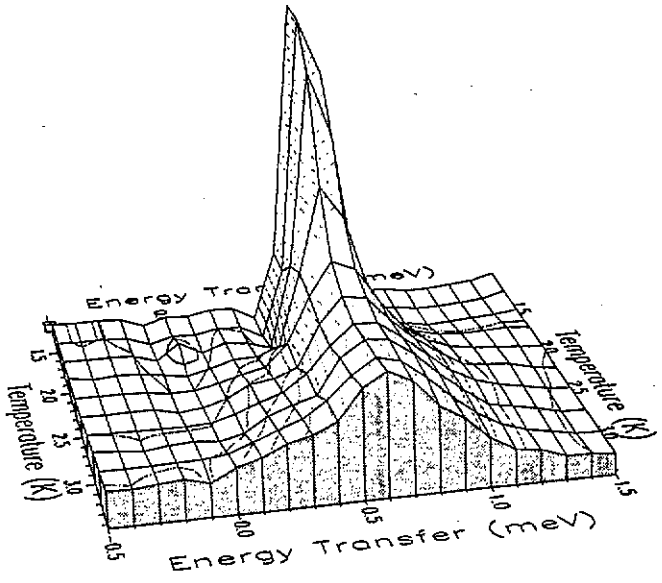

Figure 5. Three-dimensional representation of the temperature dependence of $S(Q,\omega)$ at SVP for $Q = 0.40$ Å^{-1}. $S(Q,\omega)$ at constant Q is plotted vertically with temperature and energy in the horizontal plane. The fine broken curves are contours of constant $S(Q,\omega)$.

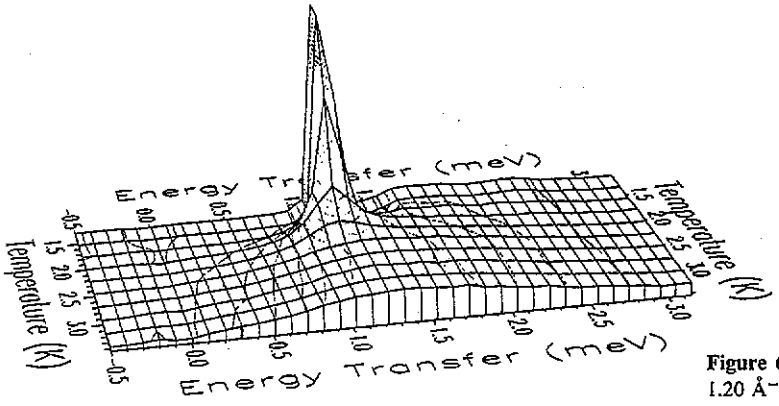

Figure 6. As figure 5 for $Q = 1.20$ Å^{-1}.

sharp peak characteristic of the superfluid (0.74 meV at $T = 1.3$ K). At all wavevectors the high-energy tail of $S(Q,\omega)$ is seen to change very little with temperature.

The individual data sets of figure 4 support these conclusions. At the smallest wavevector investigated ($Q = 0.3$ Å^{-1}, figure 4(a)) there is little evident qualitative change in peak shape on passing the lambda transition. A progressively larger effect is seen as the wavevector is increased so that at about 0.7 Å^{-1} (figure 4(a)) a sharp component of the scattering disappears at T_λ. This behaviour is also apparent at the highest wavevectors (figure 4(c)), but is most apparent around the maxon region (figure 4(b)). This wavevector-dependent temperature variation of the excitation spectrum provides support for the ideas of Glyde and Griffin (1990) and Glyde (1992) described in section 1.

In addition to these differences between small- and large-Q regions, we note the different temperature dependences above and below T_λ. Whilst there is a very rapid variation of $S(Q,\omega)$ in the superfluid phase, the scattering changes only very slowly with temperature in the normal phase. This effect is clearly evident at the wavevectors of figures 5 to 7, but is common to all wavevectors. Figure 8 presents the measured $S(Q,\omega)$ in a contour

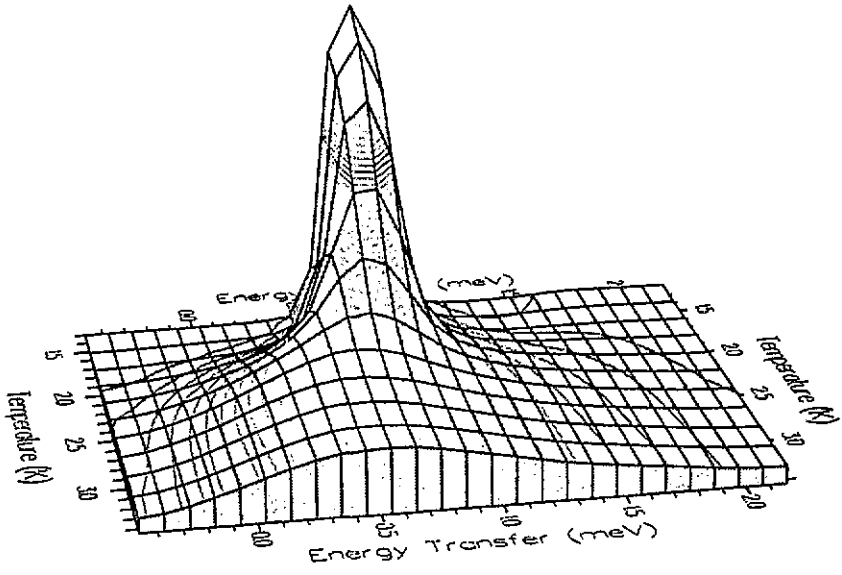

Figure 7. As figure 5 for $Q = 1.90$ Å^{-1}.

representation at four temperatures, 1.24, 2.07, 2.26 and 2.49 K. At the lowest temperature, the sharpness of the excitations is evident, as is the rapid increase in the one-phonon intensity $Z(Q)$, as observed initially by Cowley and Woods (1971). At the intermediate temperatures of this set, the rapid onset of linewidth broadening is apparent, with very wide scattering persisting above the lambda point. The excitation frequency drops most significantly with temperature in the region of the roton minimum. Once again the major changes in the scattering function are seen to occur below T_λ, with much slower changes in the normal fluid phase.

Paper II deals with various models of the excitation spectrum, as described in section 1.

5. Multiphonon spectrum

Although the existence and importance of the multiphonon continuum was recognized in the pioneering work of Cowley and Woods (1971) there has been relatively little experimental work examining this part of the excitation spectrum. The first clear sign of structure in the continuum scattering was obtained by Svensson *et al* (1976). The high-resolution measurements of Stirling (1985, 1990) demonstrated clearly that this structure could be related to the details of the one-phonon spectrum.

The present data confirm and extend previous knowledge of the continuum structure. The scattering at energies above the phonon-roton peak is seen to exhibit significant structure at low temperatures (see figure 3). This arises from the excitation of two or more phonons in a single scattering process and is determined by the multiphonon density of states and the phonon–phonon interactions. Figure 9 shows a contour map of the multiphonon region as measured in the present experiment, at $T = 1.3$ K. As in previous work (Stirling 1985, 1990) the arrows indicate the positions of twice the roton energy ($2R$), one maxon plus one roton ($M + R$), and twice the maxon energy ($2M$). At wavevector transfers below 0.7 Å^{-1} the multiphonon scattering is in the form of a single peak between $2R$ and $M + R$.

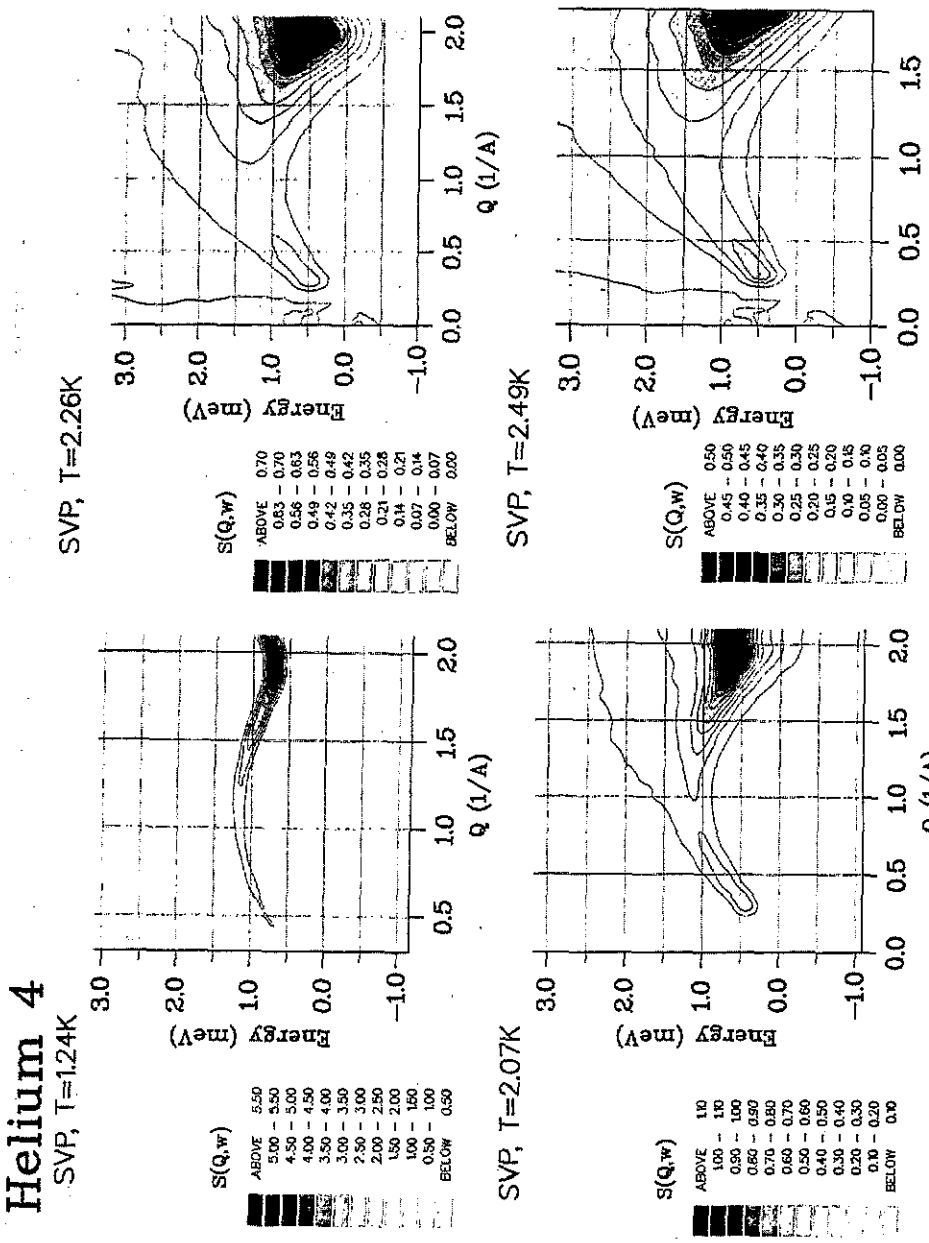

Figure 8. Contour maps of $S(Q, \omega)$ at SVP at temperatures in the superfluid (T = 1.24 K, 2.07 K) and normal (T = 2.26 K, 2.49 K) phases.

By 0.8 Å^{-1}, this has moved up to just below the $M + R$ position and a second peak of similar intensity appears near the two-maxon energy, $2M$. The peak at $2M$ increases in intensity with Q and merges with the broad peak that appears near the recoil energy at 2 Å^{-1}, without a noticeable energy shift. The peak near $M + R$, however, decreases in energy, reaching a minimum just above the two-roton energy at $Q = 1.4$ Å^{-1}, where it also displays a maximum in intensity. As Q is increased this peak is absorbed at 1.9 Å^{-1} by the emerging 'recoil' peak. The recoil peak corresponds to the scattering of a neutron from a single (nearly free) helium atom and has the dispersion relation $\hbar\omega(Q) = \hbar^2Q^2/2m_4$ (Glyde and Svensson 1987). At wavevectors beyond the collective excitation regime, only recoil scattering is observed. These conclusions are in good agreement with previous triple-axis spectrometer data (Stirling 1985, 1990). The structure in the multiphonon continuum described above is only visible at the lowest temperatures. By $T = 1.75$ K, only a single broad peak is visible above the one-phonon excitation and, at $T = 1.96$ K the structure is no longer discernible, with the scattering intensity decreasing smoothly at all wavevectors, above the sharp one-phonon peak. Figure 4 exemplifies these effects.

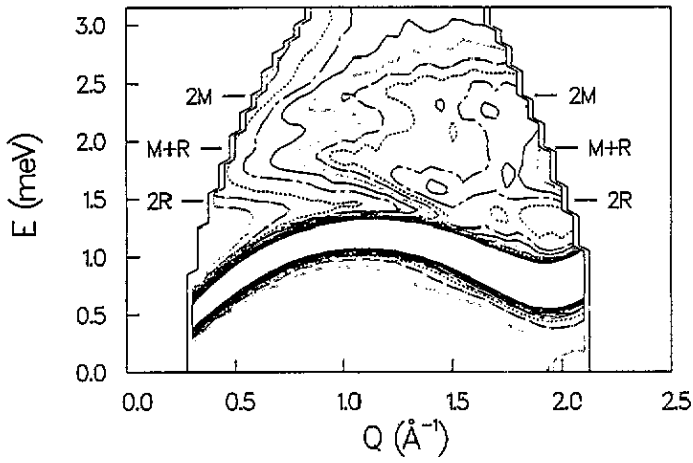

Figure 9. A contour map of $S(Q, \omega)$ in the multiphonon region at SVP at a temperature of 1.30 K. The intense single-phonon excitation is represented by the white band in the lower part of the figure. '$2R$' indicates twice the roton energy, '$2M$' is twice the maxon energy, and '$M + R$' is the sum of the maxon and roton energies. The contours represent steps of 0.01 meV^{-1} in $S(Q, \omega)$.

Raman scattering experiments (Greytak and Yan 1971) have shown the existence at low Q of a two-roton bound state of energy $2R - E_b$, where E_b is the roton binding energy. Ruvalds and Zawadowski (1970) have calculated the coupling between this and the single-phonon excitations, in order to describe the shape of the one-phonon dispersion curve for wavevectors above 2.4 Å^{-1}, where it is seen to bend over, reaching an energy of $2R$, before losing intensity and disappearing. Our measurements show no indication of a peak in $S(Q, \omega)$ at an energy between the one-phonon and the two-roton energy. The lowest-lying peak in the multiphonon spectrum does not go below $2R$ in the wavevector range of our measurements, though it may do so at low Q. This is not inconsistent with the Raman scattering measurements, which probe $S(Q, \omega)$ at Q very close to zero. Ruvalds and Zawadowski mention that the coupling constant and hence the binding energy may

be a function of Q, which introduces the possibility of the roton–roton interaction being repulsive in the wavevector region measured in the IN6 experiment, as suggested by our data. From an analysis of their neutron scattering measurements, Smith *et al* (1977) deduced that repulsive roton–roton interactions do play an important role at larger wavevectors (2.7–3.3 Å^{-1}), but this has been challenged by Tüttö and Zawadowski (1978) as being dependent on the particular analysis procedure employed. For a more complete discussion of roton–roton interactions see Bedell *et al* (1984).

Götze and Lücke (1976) and Manousakis and Pandharipande (1986) have calculated the structure of $S(Q, \omega)$ at $T = 0$ over the entire collective excitation regime. Starting with the Feynman–Cohen (1956) excitation operator, Manousakis and Pandharipande (1986) generate a set of correlated basis functions to describe the density excitations of the system. Interactions between the one-phonon and two-phonon excitations are included, which modify the one-phonon energies and produce a dispersion curve in good agreement with neutron scattering results. They also calculate the two-phonon scattering intensity, which is in good qualitative agreement with our measurements. A quantitative analysis, however, is not possible as the shape of the calculated two-phonon spectrum depends strongly on the number of self-energy terms included, and only the first three terms are used. Manousakis and Pandharipande obtain a multiphonon spectrum containing peaks which can be identified as arising from $2M$, $2R$, and $M + R$ excitations, as observed in our experiments. Götze and Lücke (1976) have also presented calculated multiphonon spectra exhibiting structure qualitatively similar to that observed experimentally.

6. Conclusion

Neutron scattering experiments have been performed to measure the dynamic structure factor $S(Q, \omega)$ of liquid ^{4}He. The data have been obtained using the time-of-flight technique, which enables us to record the structure factor over a wide range of wavevectors and energy transfers in a single measurement. The energy and wavevector scales of the spectrometer were calibrated to relative errors of less than 0.2% and 0.5%, respectively. A lengthy and careful data reduction procedure was then followed to minimize systematic errors in the measurements. We systematically examined the temperature dependence in the wavevector region $0.3 < Q < 2.1$ Å^{-1}, measuring $S(Q, \omega)$ at SVP at 15 different temperatures between 1.24 and 4.95 K, with particular emphasis on the region near T_λ.

At the lowest measured temperatures, sharp excitations are observed over the entire measured wavevector region, which are unique to superfluid ^{4}He. As the temperature is increased through the lambda point, the excitations of the linear (phonon-type) part of the dispersion curve broaden, whilst at higher wavevectors the sharp excitations disappear abruptly at T_λ. Sharp maxon and roton peaks are seen to be present only in the superfluid state. The variation of $S(Q, \omega)$ with temperature is very marked in the superfluid phase, but is almost non-existent in the normal fluid, particularly at higher Q. The temperature dependence of the sharp excitations is studied in more detail in paper II, where we compare the results for $S(Q, \omega)$ with the predictions of three models in which explicit account is taken of the temperature dependence of the excitations.

Acknowledgments

The authors are grateful to the Institut Laue–Langevin for the provision of the neutron scattering facilities used in this work; KHA acknowledges the award of an ILL studentship

and a fellowship from the Japan Society for the Promotion of Science. We thank H R Glyde for many stimulating discussions and for a critical reading of the manuscript. The expert technical assistance of Y Blanc is gratefully acknowledged. Financial support was provided by the UK Science and Engineering Research Council, by the Bundes Ministerium für Forschung und Technologie, by the North Atlantic Treaty Organisation and by Keele University. We thank R Hayler for his assistance with the preparation of the diagrams and tables.

References

Andersen K H 1991 *Thesis* Keele University
Andersen K H, Stirling W G, Scherm R, Stunault A, Fåk B, Godfrin H and Dianoux A J 1992 *Physica* B **180 & 181** 851
Bedell K, Pines D and Zawadowski A 1984 *Phys. Rev.* B **29** 102
Blanc Y 1983 *Institut Laue–Langevin Report* ILL 83BL21G
Cowley R A and Woods A D B 1971 *Can. J. Phys.* **49** 177
Donnelly R J, Donnelly J A and Hills R N 1981 *J. Low Temp. Phys.* **44** 471
Feynman R P 1954 *Phys. Rev.* **94** 262
Feynman R P and Cohen M 1956 *Phys. Rev.* **102** 1189
Glyde H R 1992 *Phys. Rev.* B **45** 7321
Glyde H R and Griffin A 1990 *Phys. Rev. Lett.* **65** 1454
Glyde H R and Svensson E C 1987 *Methods of Experimental Physics* vol 23, part B, ed D L Price and K Sköld (New York: Academic) p 303
Götze W and Lücke M 1976 *Phys. Rev.* B **13** 3825
Greytak T J and Yan J 1971 *Proc. 12th Int. Conf. Low Temperature Physics, Kyoto, Japan* ed E Kanda (New York: Academic) p 89
Griffin A 1993 *Excitations in a Bose-Condensed Liquid* (Cambridge: Cambridge University Press)
Hallock R B 1972 *Phys. Rev.* A **5** 320
Landau L D 1941 *J. Phys. USSR* **5** 71
—— 1947 *J. Phys. USSR* **11** 91
Landau L D and Khalatnikov I M 1949 *Zh. Eksp. Teor. Fiz.* **19** 637
Lovesey S W 1984 *Theory of Neutron Scattering from Condensed Matter* vol 1 (Oxford: Clarendon)
Manousakis E and Pandharipande V R 1986 *Phys. Rev.* B **33** 150
Miller A, Pines D and Nozieres P 1962 *Phys. Rev.* **127** 1452
Ruvalds J and Zawadowski A 1970 *Phys. Rev. Lett.* **25** 333
Sears V F 1975a *Nucl. Instrum. Methods* **123** 521
—— 1975b *Adv. Phys.* **24** 1
Smith A J, Cowley R A, Woods A D B, Stirling W G and Martel P 1977 *J. Phys. C: Solid State Phys.* **10** 543
Stirling W G 1985 *Proc. 2nd Int. Conf. Phonon Physics* ed J Kollar, N Kroo, N Menyhard and T Siklos (Singapore: World Scientific) p 829
—— 1990 *Physica* B **165 & 166** 501
—— 1991 *Excitations in Two-dimensional and Three-Dimensional Quantum Fluids* ed A G F Wyatt and H J Lauter (New York: Plenum) p 25
Stirling W G and Glyde H R 1990 *Phys. Rev.* B **41** 4224
Stunault A, Andersen K H, Blanc Y, Fak B, Godfrin H, Guckelsberger K and Scherm R 1992 *Physica* B **180 & 181** 926
Svensson E C, Martel P, Sears V F and Woods A D B 1976 *Can. J. Phys.* **54** 2178
Svensson E C, Sears V F, Woods A D B and Martel P 1980 *Phys. Rev.* B **21** 3638
Talbot E and Griffin A 1984 *Phys. Rev.* B **29** 2531
Talbot E F, Glyde H R, Stirling W G and Svensson E C 1988 *Phys. Rev.* B **38** 11229
Tüttö I and Zawadowski A 1978 *J. Phys. C: Solid State Phys.* **11** L385
Waller I and Frömann P O 1952 *Ark. Fys.* **4** 183
Windsor C G 1981 *Pulsed Neutron Scattering* (London: Taylor and Francis)
Woods A D B and Cowley R A 1973 *Rep. Prog. Phys.* **36** 1135
Woods A D B, Hilton P A, Scherm R and Stirling W G 1977 *J. Phys. C: Solid State Phys.* **10** L45
Woods A D B and Svensson E C 1978 *Phys. Rev. Lett.* **41** 974
Woods A D B, Svensson E C and Martel P 1978 *Can. J. Phys.* **56** 302